Response to reviewer 1's comments for Operational performance of the Vaisala CL61 ceilometer for atmospheric profiling

Viet Le[1], Ewan J. O'Connor[1], Maria Filioglou[2], and Ville Vakkari[1, 3]

[1]Finnish Meteorological Institute, Helsinki, 00101, Finland
[2]Finnish Meteorological Institute, Atmospheric Research Centre of Eastern Finland, Kuopio, Finland
[3]Atmospheric Chemistry Research Group, Chemical Resource Beneficiation, North-West University, Potchefstroom, 2520, South Africa

Correspondence: viet.le@fmi.fi

We would like to thank the reviewers for the constructive comments. Below are the reviewer comments in black text, followed by our responses in blue text. Where applicable, we also provide changes to the manuscript in *blue italics*.

1 General comments

The study by Le et al. focuses on evaluating several instrumental characteristics of the Vaisala CL61 ceilometer for aerosol vertical profiling applications. The manuscript addresses the quantification of instrumental artifacts in the measurements, in terms of bias and noise, based on several years of observations acquired both with and without a termination hood, and proposes methods to correct for these instrumental effects. In addition, the authors describe an automated calibration methodology based on liquid cloud layers and highlight signal drifts that are attributed to instrumental effects.

Overall, the manuscript is well written and allows the reader to follow most of the methodological steps taken by the authors. The topic is of considerable interest to the atmospheric remote sensing community, as this instrument - commercially available in recent years - is becoming increasingly widespread. I therefore recommend publication of the manuscript after addressing the minor comments listed below.

We would like to thank the reviewer for their positive evaluation of the manuscript.

2 Specific comments

The study refers to the difference between the background signal during daytime and nighttime conditions (e.g., Section 4.1 and Fig. 5). However, it is not entirely clear whether this difference is actually exploited to quantitatively validate the results obtained with more accurate measurements (e.g., those acquired with the termination hood). For sites or networks where the termination hood is not available, could nighttime measurements under pristine conditions be considered a reasonable proxy for estimating instrumental noise (without solar background)?

The following has been added to Sect. 3.1

In principle, the nighttime measurements could be used to estimate $P_{\text{instrument}}$. However, only the portion of the $P_{\text{instrument}}$ profile at higher ranges, where clouds and aerosols are absent, can be reliably estimated. An example is shown in Fig. S2 in the Supplement, where σ^2_{ppol/r^2} agrees well between the hood termination and nighttime measurements only at ranges above approximately 2 km. This agreement is observed only under clear-sky conditions, as cloud layers at lower ranges can increase the measured values.

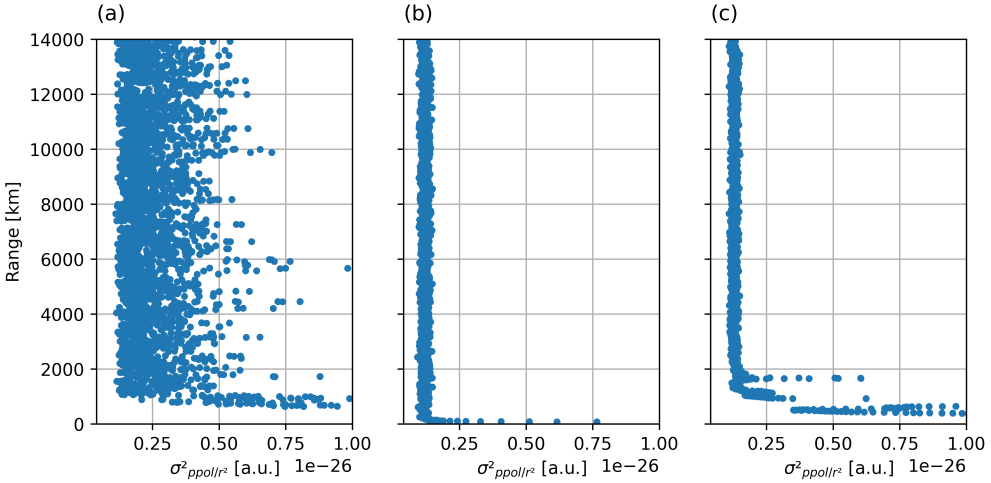

Figure S2. *Example of σ^2_{ppol/r^2} profile in Kenttärova during a) a cloudy night on 2024-03-05 00:00 to 02:00 UTC, b) termination hood measurement on 2024-03-05 14:00 to 15:00 UTC, c) a clear-sky night on 2024-03-06 20:00 to 22:00 UTC.*

Firmware corrections: it may be useful to provide additional details—within the limits of the manufacturer's documentation—on how the firmware attempts to compensate for both the background signal and sensitivity variations (i.e., calibration coefficient). For instance, is a test LED used for internal monitoring of sensitivity changes? How is the firmware compensation handled during measurements performed with the termination hood?

To our knowledge, no test LED is included in the setup. For the termination hood measurement, no information is passed on to the instrument hardware, so the measurements are continued exactly as during usual atmospheric observations. This is why the termination hood can be used to quantify instrumental performance and bias in the near range.

The following are included in the text regarding the firmware:

...and C_L represents the lidar constant. This constant encapsulates the system-specific characteristics of the lidar, such as its receiver optics and laser properties. It is initially determined and provided by the manufacturer, but it may drift over time as the instrument ages and its performance changes. Although the internal firmware attempts to monitor and compensate for these changes, additional calibration, such as absolute calibration using stratocumulus clouds, is still necessary...

...The hood was applied without modifying the instrument's internal operating parameters, ensuring that all measurements reflected normal operational conditions...

σ_R: the approximation introduced at line 245 and in Eq. (31) appears to be dimensionally inconsistent. β_p is expressed in $\mathrm{m}^{-1}\ \mathrm{sr}^{-1}$, whereas R is defined as a ratio between two backscatter coefficients. Could this be a typographical error?

Thank you, this has been fixed.

Assuming σ_{β_m} and σ_{δ_m} are negligible and approximating $\sigma_R \approx \frac{\sigma_{\beta_p}}{\beta_m}$, this reduces to

$$\sigma^2_{\delta_p} \approx \left(\frac{\partial \delta_p}{\partial \delta_v}\sigma_{\delta_v}\right)^2 + \left(\frac{\partial \delta_p}{\partial R}\frac{\sigma_{\beta_p}}{\beta_m}\right)^2. \quad (1)$$

Additional instrumental effects not explicitly addressed:

a) The manuscript mentions the issue of overlap and refers to a correction methodology (Hervo et al., 2016), but this correction is not applied in the present analysis. Do the authors believe that the same technique developed for the CHM-15k could also be applied to the CL61 in order to separate the overlap contribution from other instrumental effects?

Hervo et al., 2016 is an example of how the internal temperature could affect the measurements. In this work, we demonstrated that the instrumental background bias and noise are also temperature dependent, and we presented a method for bias correction and uncertainty estimation based on the background characteristics.

b) Another issue not mentioned in the manuscript, which affected previous models of Vaisala ceilometers, is absorption by water vapor. According to the manufacturer, this issue has been mitigated by selecting a different wavelength and a very narrow bandwidth. Have the authors had the opportunity to verify this aspect in their measurements?

The finding by Looschelders et al. (2025) that calibration factors vary by less than 5% between CL61 instruments, coupled with the absence of seasonality in the calibration factor across all sites in this study (Fig. 6), indicate that the effect of water vapor is likely negligible on CL61.

Furthermore, we quantified the effect of water vapor absorption on CL61 by using the HITRAN molecular absorption database (Gordon et al., 2026). We compared two lidar systems: the CL51 with the emitted wavelength of 910 ± 1.44 nm (Wiegner and Gasteiger, 2015), and the CL61 with the emitted wavelength of 910.55 ± 0.08 nm, where the reported uncertainties correspond to the standard deviation ($\pm\sigma$) assuming Gaussian distributions. It should be noted that the information about the CL61 wavelength is not officially published, but only obtained through personal communication. Additionally, the transmitter from CL61 is identical to the non-water channel transmitter from the Vaisala DIAL lidar (personal communication) which operates at the same 910.55 nm wavelength, while its water channel is operating at a nearby wavelength of 910.99 nm (DA10 User Guide: https://docs.vaisala.com/r/M212895EN-E/en-US, last access: 10 June 2026). This further supports the much narrower width of the emission spectrum of CL61 compared to CL51. Given these assumptions, our analysis indicates that water vapor absorption reduces the two-way transmission in the CL51 by approximately a factor of 10 more than in the CL61. As the impact of atmospheric water vapor on the CL51 has previously been reported (Wiegner and Gasteiger, 2015), this result indicates that the effect of atmospheric water vapor absorption is minimal on the CL61.

3 Technical comments

Nomenclature: the CL61 is referred to both as a "ceilometer" and as an "elastic backscatter lidar" (e.g., line 1), seemingly interchangeably. In recent years, the term "Automatic Lidar-Ceilometer" has become increasingly common. The authors may wish to consider this terminology.

Thanks, this has been implemented.

Abstract: the first part mainly uses present tense verbs, whereas the second part switches to past tense. The authors may consider harmonizing the tense throughout the abstract.

The abstract has been updated:

The Vaisala CL61 is a new generation elastic backscatter lidar that extends conventional Automatic Lidar-Ceilometer capabilities by providing depolarization ratio measurements. Reliable use of these measurements, however, requires thorough evaluation and characterisation of the instrument performance and subsequent corrections applied. In this study, performance of multiple CL61 instruments across different sites over 3 years period have been assessed. Results indicate some differences between instruments, with most of these early production units exhibiting a pronounced decrease in laser power over time, accompanied by an increase in background noise likely due to weaker return signal. Normally, the instrument scales the internal calibration factor to compensate for changes in laser power and thus provide consistent attenuated backscatter coefficient values from profile to profile over time. However, for the instrument at the Lindenberg site, by performing manual calibration with atmospheric targets it is noted that once the laser power dropped below 40% *there is no further compensation in the internal calibration factor.*

The instrumental background noise and bias, characterized using the termination hood, are found to vary with temperature. A method has been developed for correcting the instrumental bias and for estimating the associated uncertainty. Additionally, an approach to estimate the uncertainty of volume and particle backscatter and linear depolarization ratio is presented. In a case study representing low aerosol load condition in Finland, the bias-corrected particle linear depolarization ratio has been found to deviate by up to 0.1 from the original instrument-provided volume linear depolarization ratio. This demonstrates the importance of accounting for the molecular contribution in both volume backscatter and linear depolarization ratio when quantitatively interpreting aerosol measurements by the CL61 Automatic Lidar-Ceilometer operating at the wavelength of $910.55\ \mathrm{nm}$. *Finally, signal loss in one unit has been traced to fogging of the inside surface of the window, and attributed to insufficient internal heating linked to the instrument's firmware behavior.*

Line 4: can background noise appropriately be referred to as a "signal"? In addition, two rather different issues are mentioned consecutively: the quantification of background noise and calibration using liquid clouds. It might be better to separate these two aspects more clearly.

Thanks, the correct term "background noise" has been used. As recommended also by the Reviewer 2, the methodological details, namely the quantification of background noise and the calibration using liquid clouds, have been removed from this section to place greater focus on the results.

In this study, performance of multiple CL61 instruments across different sites over 3 years period have been assessed. Results indicate some differences between instruments, with most of these early production units exhibiting a pronounced decrease in laser power over time, accompanied by an increase in background noise likely due to weaker return signal.

Line 4: “long-term behavior” is somewhat generic and could be specified more precisely. The same applies to “variability” in line 5.

Changed “long-term behavior” to ”performance .. over 3 years” and ”variability” to ”differences”. See the answer above.

Lines 12–14: the approach used for aerosol inversion and the calculation of the depolarization ratio are not entirely novel. Rather, the contribution of the paper could be emphasized in terms of the uncertainty propagation in the inversion and in the depolarization ratio retrieval.

We have modified lines 12–14 as following:

A method has been developed for correcting the instrumental bias and for estimating the associated uncertainty. Additionally, an approach to estimate the uncertainty propagation of volume and particle backscatter and linear depolarization ratio is presented.

Line 14: after “accounting for molecular contribution”, it would be clearer to add “both in the aerosol backscatter and in the depolarization ratio”.

This demonstrates the importance of accounting for the molecular contribution in both backscatter and linear depolarization ratio when qualitatively interpreting aerosol measurements by the CL61 Automatic Lidar-Ceilometer operating wavelength of $910.55\ \mathrm{nm}$

Line 50: does the “optical path” referred to here correspond to the optical path inside the instrument?

We changed it to "temperature sensitivity of the instrumental background" to encompass both the optical and the electronics.

Our analysis focuses on the impact of laser power on signal quality, the temperature sensitivity of the instrumental background and methods for its correction.

Equations (1), (2), and (3): in Eq. (1), defining B as the background noise appears correct. However, in the subsequent equations, if p_{pol} and x_{pol} represent the signals provided by the instrument firmware, then B should represent the firmware estimate—rather than the exact value—of the background noise, as described in the following sections.

Thank you, this has been implemented. Instrument estimated background noise $B_{estimate}$ and residual background noise B_{res} have been introduced. Line 91 has been modified as:

where $B_{\mathrm{estimated}}$ *is the internally estimated background signal by the instrument.*

Line 100 to 105 has been modified as:

Although the instrument already determines and performs the background correction internally, residual background components may still remain in the measured signal, such as the dark signal observed during termination hood measurements (see Sect 3.1.1). Therefore, we extend Eqs. 2 and 3 to account for the residual background signal (hereafter referred to as the background signal), B_{res}*, that is not removed by the internal correction:*

Section 3.1: it might be clearer to title the section “Residual background noise”, since a first correction is already applied by the firmware. Similarly, in line 103, it might be useful to specify “unaccounted background terms”.

Thanks for the suggestion, the title of the section has been modified to "Residual background noise". See the previous reply for the additional introduction of $B_{estimate}$ and B_{res}.

Line 97: please specify what the two letters "bk" stand for, given that B already denotes "background".

Thank you, "bk" has been removed and B has been separated as instrument estimated background noise $B_{estimate}$ and residual background noise B_{res}. See previous reply for more detail

Lines 110–115: does this description uniquely (and reproducibly) define the procedure followed? In particular, the exact PyWavelets wavelet identifier (e.g., bior1.1), the definition of the minimax threshold and the method used for noise variance estimation, the treatment of approximation coefficients, and the exact threshold computation used for noise-gate identification should be clarified.

The text in lines 110–115 provides sufficient detail to reproduce the method. The minimax threshold is applied in the wavelet decomposition to reduce noise in the signal by minimizing the maximum mean squared error across the wavelet coefficients. Both the threshold computation and the wavelet decomposition can be readily implemented using PyWavelets python package following the described procedure.

The following has been added:

The mean and variance of the background are computed from the original, non-averaged data with the identified background range gates using 5-minute time intervals and 2 km range-bin intervals.

Line 133: if I am not mistaken, the terms μ have not been introduced previously and should therefore be defined.

These terms have been introduced as following in line 130:

During daylight hours, solar radiation significantly increases the variance ($\sigma^2{}_{\parallel P_{\text{res}}}$ and $\sigma^2{}_{\perp P_{\text{res}}}$) of the background signal, resulting in a daytime variance much higher than that observed at night, as shown in panels (g) and (h). Above the aerosol and cloud layers, both the mean ($\mu_{\parallel P_{\text{res}}}$ and $\mu_{\perp P_{\text{res}}}$) and variance of the background signals in both polarizations remain relatively stable with range, or at least exhibit considerably smaller variations compared to the diurnal fluctuations.

Figure 3, caption: the caption reports σ_{ppol}/r^2, whereas the axis in the figure shows σ^2_{ppol}/r^2.

Thank you, the figure axis labeled has been corrected as σ^2_{ppol/r^2}

Line 149: when referring to the instrument temperature, in what part of the instrument is it measured? It should be clarified whether this corresponds to the module temperature, the internal temperature, or specifically the laser temperature.

Thank you, this has been implemented.

To quantify the effect of temperature, the termination hood measurement was repeated over a range of internal temperatures T, reported as `internal_temperature` *in the instrument housekeeping data, across a two-year period.*

Section 3.1.2: please clarify whether the calculation of P_{solar} is performed for each individual profile.

This is performed for each individual profile.

Here, $\sigma^2_{P_{atmosphere}}$ is independent of the range and is obtained separately for each polarization in each individual profile.

Line 155: is σ^2 uniform, or σ^2/r^2?

$\sigma^2{}_{P_{atmosphere}}$ is uniform which is the $\sigma^2{}_{\frac{ppol}{r^2}}$ and $\sigma^2{}_{\frac{xpol}{r^2}}$ in the background range gates.

Line 162: I believe the reference should be to Figs. 3b and 3c, rather than 2b/2c.

Thank you for spotting the mistake, this has been fixed

Lines 205–209: additional detail may be helpful here. How is the example profile selected? Presumably the cross-correlation accounts for possible shifts in cloud altitude (or other profile characteristics)? Which exact quantity is correlated along the profile (e.g., β')?

This has been reformulated to include more details:

A methodology was developed to identify suitable liquid cloud profiles. First, a representative liquid cloud profile containing a single liquid cloud layer and exhibiting complete signal attenuation approximately 200 m above the cloud base was selected as the reference profile. Each ppol profile in the dataset was then cross-correlated with this reference to quantify their similarity. For each time step, the height corresponding to the maximum cross-correlation value was identified as the most similar location and treated as a pseudo in-cloud height. Next, the ratio of total in-cloud β', calculated over a 150 m layer centered at the pseudo in-cloud height, to the integrated β' of the entire profile was computed. A profile was classified as containing a liquid cloud if this ratio exceeded 90%, ensuring that the integrated β' was not significantly influenced by strong aerosol loading or precipitation. Additionally, the cross-correlation value at the identified height was required to exceed 5×10^{-7}. This threshold was selected to ensure that at least 1000 valid data points were available for each month.

Line 252: it might be useful to specify that the normalization assumes Poisson statistics.

Thanks, this has been implemented

Figure 4 shows the time series of background noise (variance of the background signal), normalized by integration time assuming Poisson statistics ($\sigma^2_{ppol/r^2} \times t_{intergration}$), alongside the laser power.

Sections 4.2 and 4.3: in the description of the figures (e.g., line 282 onward; line 311 onward), the text refers to station names. However, if the reader wants to identify the corresponding panel, they must read the figure caption and match the station name with the subfigure label (a, b, c, . . .). It would be more convenient either to refer directly to the subfigure in the main text or to include the station name in each subfigure title.

Thanks, this has been implemented to include the station name.

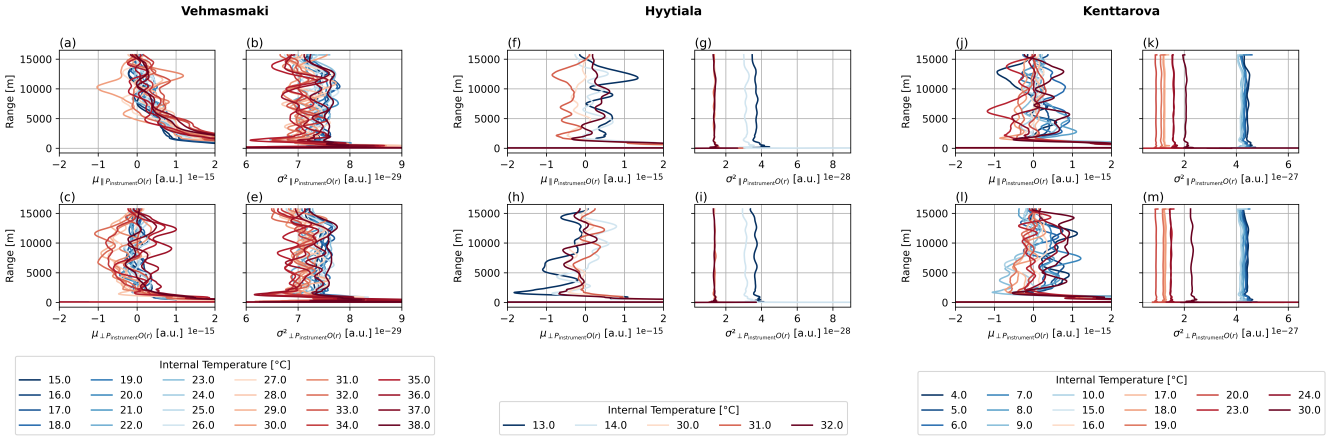

Figure 6. *Termination hood profiles at various internal temperatures (color-coded) across different sites. In Vehmasmaki: a) $\mu_{\parallel} P_{\text{instrument}} O(r)$, b) $\sigma_{\parallel} P_{\text{instrument}} O(r)$, c) $\mu_{\perp} P_{\text{instrument}} O(r)$, and d) $\sigma_{\perp} P_{\text{instrument}} O(r)$. In Hyytiala: f) $\mu_{\parallel} P_{\text{instrument}} O(r)$, g) $\sigma_{\parallel} P_{\text{instrument}} O(r)$, h) $\mu_{\perp} P_{\text{instrument}} O(r)$, and i) $\sigma_{\perp} P_{\text{instrument}} O(r)$. In Kenttärova: j) $\mu_{\parallel} P_{\text{instrument}} O(r)$, k) $\sigma_{\parallel} P_{\text{instrument}} O(r)$, l) $\mu_{\perp} P_{\text{instrument}} O(r)$, and m) $\sigma_{\perp} P_{\text{instrument}} O(r)$*

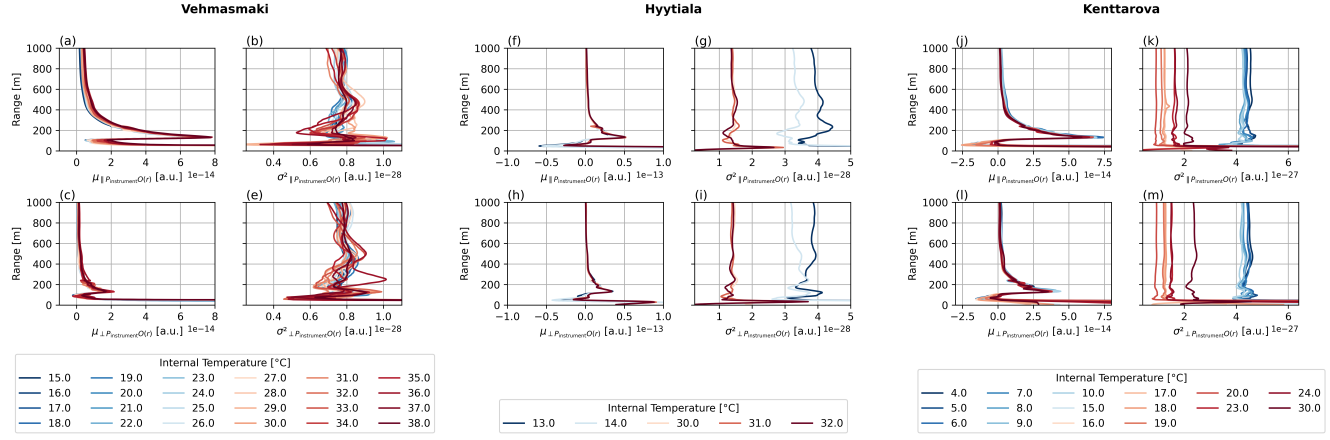

Figure 7. *Termination hood profiles at various internal temperatures (color-coded) across different sites only up to* 1000 m *range. In Vehmasmaki: a) $\mu_{\parallel} P_{\text{instrument}} O(r)$, b) $\sigma_{\parallel} P_{\text{instrument}} O(r)$, c) $\mu_{\perp} P_{\text{instrument}} O(r)$, and d) $\sigma_{\perp} P_{\text{instrument}} O(r)$. In Hyytiala: f) $\mu_{\parallel} P_{\text{instrument}} O(r)$, g) $\sigma_{\parallel} P_{\text{instrument}} O(r)$, h) $\mu_{\perp} P_{\text{instrument}} O(r)$, and i) $\sigma_{\perp} P_{\text{instrument}} O(r)$. In Kenttärova: j) $\mu_{\parallel} P_{\text{instrument}} O(r)$, k) $\sigma_{\parallel} P_{\text{instrument}} O(r)$, l) $\mu_{\perp} P_{\text{instrument}} O(r)$, and m) $\sigma_{\perp} P_{\text{instrument}} O(r)$.*

Lines 292–293: if I am not mistaken, the temperature dependence in subfigures 6k and 6m appears to reverse at some point. Are the authors able to explain this inversion?

200 Yes, it is due to the noise introduced by the internal heater when the internal temperature falls below an instrument-specific threshold (15 °C for Hyytiälä and Kenttärova). The following has been added to the text.

These instrumental background noise profiles show a pronounced sensitivity to internal temperature (from 4°C to 38°C). Notably, very low temperatures are associated with elevated instrumental background noise across the entire measurement range. This can be explained by the effect of the internal heater. As the internal temperature falls below an instrument-specific threshold (15 °C for Hyytiälä and Kenttärova), the internal heater is turned on. This leads to an increase in $\sigma^2_{P_{\text{instrument}}O(r)}$*, with the effect becoming more pronounced as the temperature decreases. When the internal temperature is high and the internal heater is off, internal temperature positively correlates with* $\sigma^2_{P_{\text{instrument}}O(r)}$.

Figure 6: the subfigures do not appear to be vertically aligned.

Thanks, this has been fixed, see the reply above.

Line 339: the quantities referred to as "values" are actually differences, correct?

Thanks, "values" has been changed to difference.

In below $1000\ \text{m}$ *range, the corrected* β'_v *differs only slightly from the original uncorrected* β'*, with the difference ranging from* 1×10^{-9} *to* $2.5 \times 10^{-9}\ \text{sr}^{-1}\ \text{m}^{-1}$

Lines 351–354: is there a physical reason why σ_δ depends on signal intensity, whereas this does not appear to be the case for σ_β? Could the authors provide an intuitive explanation?

The uncertainties of $xpol$ and $ppol$ are of the same order of magnitude. However, the absolute values of $ppol$ are much larger than those of $xpol$. As a result, the small uncertainty in $xpol$ can lead to a relatively large uncertainty in δ. The figure has been updated with an improved color scale for better visualization. Additionally, the uncertainty propagation for β now includes a 10% uncertainty associated with the calibration factor, which further increases σ_δ depending on the signal intensity.

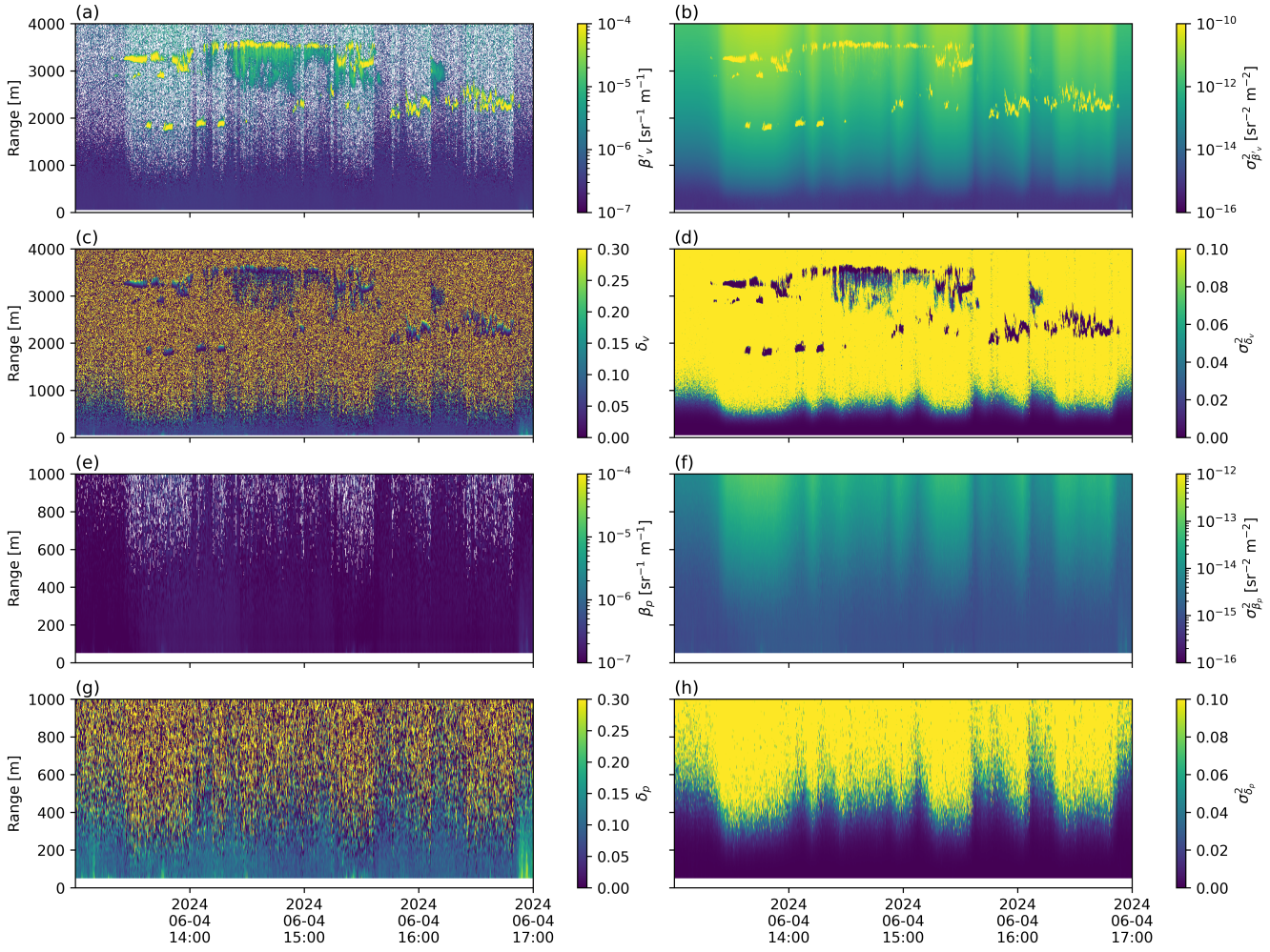

Figure 11. *An example of corrected profile in Kenttärova on 2024-06-04 13:00 - 17:00 UTC (same day as Fig. 10). a) β'_v, b) $\sigma^2_{\beta'_v}$ c) δ_v, d) $\sigma^2_{\delta_v}$ e) β_p, f) $\sigma^2_{\beta_p}$, g) δ_p, and h) $\sigma^2_{\delta_p}$.*

Lines 368–369: could the authors indicate how the blower and heater are configured to remain permanently on?

The blower and heater cannot be configured to remain permanently on.

This issue could be mitigated by keeping both the window blower and heater always on. However, at the time of this writing, this is not possible (personal communication with Vaisala).

Figure 11: how does relative humidity (RH) behave inside the instrument under these conditions?

Thanks, this has been added to the graph. The relative humidity was at below 70%. However, because the outside temperature was much colder and the window blower heater was turned off, condensation formed on the inside surface of the window.

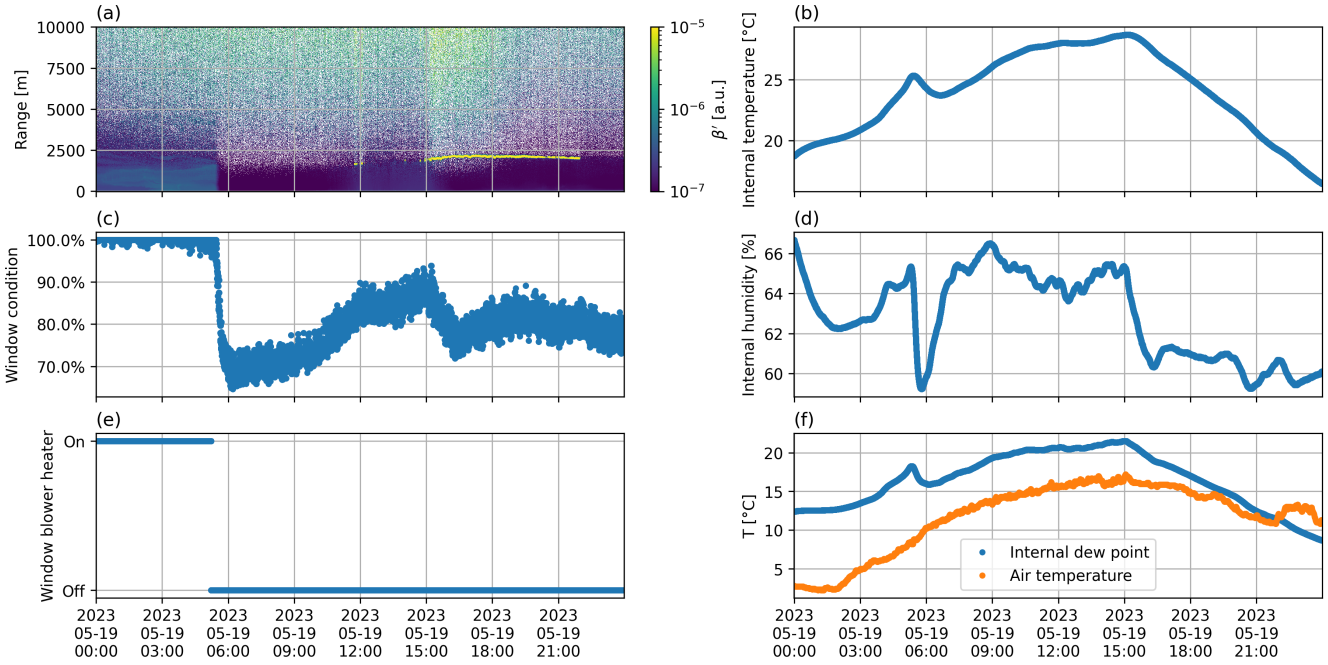

Figure 12. *Measurements from Vehmasmäki on 2023-05-19 a) β', b) Internal temperature, c) window condition, d) Internal humidity, e) Window blower heater, f) Calculated dew point and measured outside air temperature*

Conclusions: Lines 372–373: please clarify what results are specific to the CL61.

In this study, we quantify the temporal variability of background noise and calibration factors for the CL61 across multiple sites over a three-year period using methodologies adapted from existing approaches.

Line 381: since the Klett inversion depends on the signal at lower altitudes, measurements affected by the discussed issue should probably be discarded or replaced (e.g., with the immediately higher range gates) not only in the final results but also within the inversion calculation itself.

This has been added to the method:

The first 50 m range has been discarded due to unreliable data (see Sect. 4.5), and it has been demonstrated that the resulting loss in optical depth for ignoring near range gates is negligible (Wiegner and Geiß, 2012).

References

Gordon, I. E., Rothman, L. S., Hargreaves, R. J., Gomez, F. M., Bertin, T., Hill, C., Kochanov, R. V., Tan, Y., Wcisło, P., Makhnev, V. Y., Bernath, P. F., Birk, M., Boudon, V., Campargue, A., Coustenis, A., Drouin, B. J., Gamache, R. R., Hodges, J. T., Jacquemart, D., Mlawer, E. J., Nikitin, A. V., Perevalov, V. I., Rotger, M., Robert, S., Tennyson, J., Toon, G. C., Tran, H., Tyuterev, V. G., Adkins, E. M., Barbe, A., Bailey, D. M., Bielska, K., Bizzocchi, L., Blake, T. A., Bowesman, C. A., Cacciani, P., Čermák, P., Császár, A. G., Denis, L., Egbert, S. C., Egorov, O., Ermilov, A. Y., Fleisher, A. J., Fleurbaey, H., Foltynowicz, A., Furtenbacher, T., Germann, M., Guest, E. R., Harrison, J. J., Hartmann, J. M., Hjältén, A., Hu, S. M., Huang, X., Johnson, T. J., Jóźwiak, H., Kassi, S., Khan, M. V., Kwabia-Tchana, F., Lee, T. J., Lisak, D., Liu, A. W., Lyulin, O. M., Malarich, N. A., Manceron, L., Marinina, A. A., Massie, S. T., Mascio, J., Medvedev, E. S., Meshkov, V. V., Mellau, G. C., Melosso, M., Mikhailenko, S. N., Mondelain, D., Müller, H. S. P., O'Donnell, M., Owens, A., Perrin, A., Polyansky, O. L., Raston, P. L., Reed, Z. D., Rey, M., Richard, C., Rieker, G. B., Röske, C., Sharpe, S. W., Starikova, E., Stolarczyk, N., Stolyarov, A. V., Sung, K., Tamassia, F., Terragni, J., Ushakov, V. G., Vasilchenko, S., Vispoel, B., Vodopyanov, K. L., Wagner, G., Wójtewicz, S., Yurchenko, S. N., and Zobov, N. F.: The HITRAN2024 molecular spectroscopic database, Journal of Quantitative Spectroscopy and Radiative Transfer, 353, 109 807, https://doi.org/10.1016/j.jqsrt.2026.109807, 2026.

Looschelders, D., Christen, A., Grimmond, S., Kotthaus, S., Fenner, D., Dupont, J.-C., Haeffelin, M., and Morrison, W.: Inter-Instrument Variability of Vaisala CL61 Lidar-Ceilometer's Attenuated Backscatter, Cloud Properties and Mixed-Layer Height, Meteorological Applications, 32, e70 088, https://doi.org/10.1002/met.70088, _eprint: https://rmets.onlinelibrary.wiley.com/doi/pdf/10.1002/met.70088, 2025.

Wiegner, M. and Gasteiger, J.: Correction of water vapor absorption for aerosol remote sensing with ceilometers, Atmospheric Measurement Techniques, 8, 3971–3984, https://doi.org/10.5194/amt-8-3971-2015, publisher: Copernicus GmbH, 2015.

Wiegner, M. and Geiß, A.: Aerosol profiling with the Jenoptik ceilometer CHM15kx, Atmospheric Measurement Techniques, 5, 1953–1964, https://doi.org/10.5194/amt-5-1953-2012, 2012.